iJRASET
International Journal For Research in Applied Science and Engineering Technology

INTERNATIONAL JOURNAL FOR RESEARCH

IN APPLIED SCIENCE & ENGINEERING TECHNOLOGY

Volume: 7 **Issue:** II **Month of publication:** February

DOI: http://doi.org/10.22214/ijraset.2019.2015

www.ijraset.com

Call: 08813907089 | E-mail ID: ijraset@gmail.com

International Journal for Research in Applied Science & Engineering Technology (IJRASET)
ISSN: 2321-9653; IC Value: 45.98; SJ Impact Factor: 6.887
Volume 7 Issue II, Feb 2019- Available at www.ijraset.com

Study of a Convective Heat Transfer, Modelling and Prediction in 2-D Nozzle for Compressible Flow

B Dharshan[1], Ritesh Kumar[2]
[1, 2] *Bachelor Student, Department of Aeronautical Engineering, Acharya Institute of Technology, Bangalore-560107*

Abstract: ***The increase in the quantification of all critical variables involved in the construction of a nozzle has led to the increase in the number of trial and error during the experiments. At this stage, the rapid growth in the field of computational science has made construction of flow related models, using modern computer languages and mathematical models efficient and accurate. The study here involves modelling of 3 bi-laterally symmetrical, variable throat-to-inlet diameter ratio nozzles, analysing the flow through the nozzle and simultaneously performing a grid independent study to compare the corresponding variation in the parameters using ANSYS Fluent. The later stage involves exporting the output variables obtained to an open source, statistical computing program known as R-Studio. Using the pre-defined built in function and the imported data, the prediction and optimization is formulated on 3 different types of nozzle.***
Keywords: Prediction, Optimization, Throat-to-diameter ratio, Linear regression, Multiple regression, Mach number, Static temperature, Dynamic pressure, Path lines, Turbulence model, Grid independent study, Density, Velocity, Contours .

I. INTRODUCTION

A typical nozzle is constructed in such a manner where, the primary objective of any type of nozzle is to vary the flow with them. They are primarily used to generate required amount of velocity by expanding the combustion gases produced by burning of propellants. The inlet section of the nozzle as shown in fig. has lesser value of velocity and this velocity is exponentially increased at the later stage, past the throat section. Hence the major changes which occur in a nozzle are at the throat section of the nozzle and this variation also depends on the ratio of throat-to-inlet diameter. The chocked flow is where the mass flow will not increase with a further decrease in the downstream pressure environment while upstream pressure is fixed, where the limiting parameter is velocity.

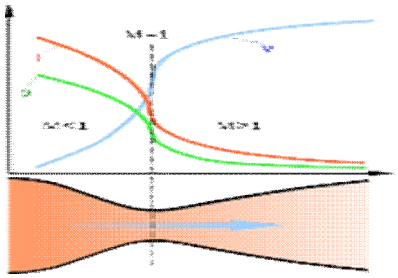

Fig.1.1 Flow parameter variation in a typical nozzle

The prediction of the variation of the variables such as temperature, pressure and velocity at the throat section of the nozzle becomes vital for the designing and for the performance of the nozzle at critical conditions. The case study performed by L.H Back - Flow in a planar convergent divergent nozzle and convective heat transfer 2009 [1] , Effect of nozzle geometry on local convective heat transfer-D.W. Colucci, R. Viskanta 1996 [2] gives broader idea about the effects of sudden change in the nozzle geometry give rise to a sudden change in the flow parameters.

II. METHODOLOGY

The methodology is basically divided into 2 main components, where the primary stage involves the use of ANSYS Fluent to create geometry according to the problem specification, analyse the flow through the nozzle and export the values obtained from the analysis to R-Studio.
The secondary stage, involves importing the data from the analysis and performing various built in function operation on them to predict and optimize the data. Fig. 2.1 shows the flow chart for the overall procedure followed.

ISSN: 2321-9653; IC Value: 45.98; SJ Impact Factor: 6.887
Volume 7 Issue II, Feb 2019- Available at www.ijraset.com

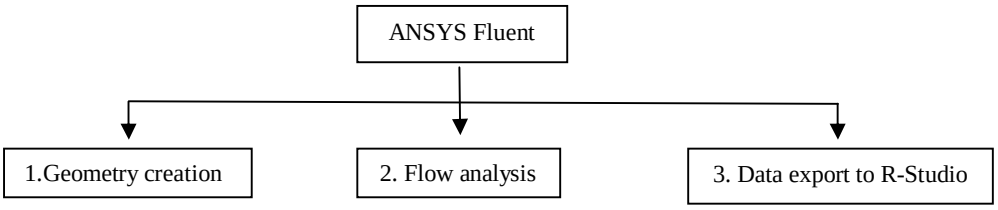

Fig.2.1 Flow chart for ANSYS Fluent operation

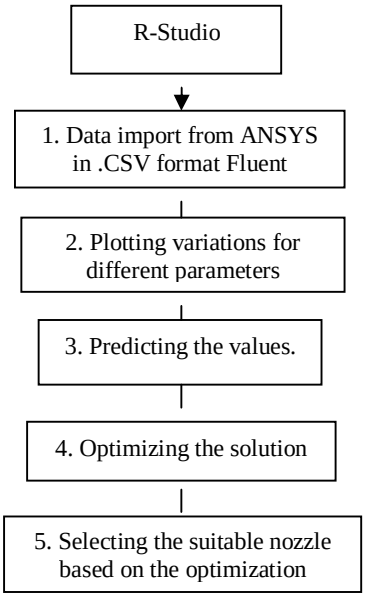

Fig.2.2 Flow chart for R-Studio operation

III.ANSYS GEOMETRY AND ANALYSIS

A. Problem specification.

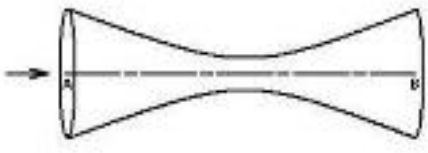

Fig. 3.1 Basic diagram for the problem specification

From fig. 3.1 let the air flowing at a very high speed through a convergent-divergent nozzle having a circular cross sectional area A. Let it vary with respect to the axial distance from the throat as x. Formulating this variation of cross-sectional are with respect to x:

$A = 0.1 + x^{2;}$ where x varies from -0.5 to +0.5. (1)

Where *A* is in square meters and *x* is in meters. The stagnation pressure p_o at the inlet is 101,325 Pa., the stagnation temperature T_o and The static pressure *p*. We will calculate the Mach number, pressure and temperature distribution in the nozzle using FLUENT and compare the solution to quasi-1D nozzle flow results. The Reynolds number for this high-speed flow is large. So we expect viscous effects to be confined to a small region close to the wall. So it is reasonable to model the flow as inviscid.

The construction of the geometry involves the construction of basically 3 different types of nozzle having different throat-to-inlet diameter ratio. The detail description regarding the values for the construction of nozzles is tabulated in table 3.1.

Table 3.1

Nozzle	Ratio of throat-to-inlet diameter
Nozzle -1	0.53
Nozzle -2	0.40
Nozzle -3	0.475

The construction of all the three nozzles are carried out using co-ordinate system and the co-ordinate points for each nozzle is shown in table 2, table3 and table 4.

Integer group	Integer ID	x	y	z
1	1	-0.5	0.33	0
1	2	-0.45	0.31	0
1	3	-0.4	0.28	0
1	4	-0.35	0.26	0
1	5	-0.3	0.24	0
1	6	-0.25	0.22	0
1	7	-0.2	0.21	0
1	8	-0.15	0.19	0
1	9	-0.1	0.187	0
1	10	-0.05	0.180	0
1	11	0	0.17	0
1	12	0.05	0.180	0
1	13	0.1	0.187	0
1	14	0.15	0.19	0
1	15	0.2	0.21	0
1	16	0.25	0.22	0
1	17	0.3	0.24	0
1	18	0.35	0.26	0
1	19	0.4	0.28	0
1	20	0.45	0.31	0
1	21	0.5	0.33	0
2	1	0.5	0.333	0
2	2	0.5	0	0
3	1	0.5	0	0
3	2	-0.5	0	0
4	1	-0.5	0	0
4	2	-0.5	0.333	0

Table 2 Co-ordinates for Nozzle 1

Integer group	Integer ID	x	y	z
1	1	-0.5	0.30	0
1	2	-0.45	0.28	0
1	3	-0.4	0.25	0
1	4	-0.35	0.23	0
1	5	-0.3	0.21	0
1	6	-0.25	0.18	0
1	7	-0.2	0.16	0
1	8	-0.15	0.15	0
1	9	-0.1	0.13	0
1	10	-0.05	0.129	0
1	11	0	0.124	0
1	12	0.05	0.129	0
1	13	0.1	0.13	0
1	14	0.15	0.15	0
1	15	0.2	0.16	0
1	16	0.25	0.18	0
1	17	0.3	0.21	0
1	18	0.35	0.23	0
1	19	0.4	0.25	0
1	20	0.45	0.28	0
1	21	0.5	0.30	0
2	1	0.5	0.30	0
2	2	0.5	0	0
3	1	0.5	0	0
3	2	-0.5	0	0
4	1	-0.5	0	0
4	2	-0.5	0.30	0

Table 3 Co-ordinates for Nozzle 2

Integer group	Integer ID	x	y	z
1	1	-0.5	0.32	0
1	2	-0.45	0.29	0
1	3	-0.4	0.27	0
1	4	-0.35	0.25	0
1	5	-0.3	0.22	0
1	6	-0.25	0.20	0
1	7	-0.2	0.19	0
1	8	-0.15	0.17	0
1	9	-0.1	0.16	0
1	10	-0.05	0.157	0
1	11	0	0.154	0
1	12	0.05	0.157	0
1	13	0.1	0.16	0
1	14	0.15	0.17	0
1	15	0.2	0.19	0
1	16	0.25	0.20	0
1	17	0.3	0.22	0
1	18	0.35	0.25	0
1	19	0.4	0.27	0
1	20	0.45	0.29	0
1	21	0.5	0.32	0
2	1	0.5	0.32	0
2	2	0.5	0	0
3	1	0.5	0	0
3	2	-0.5	0	0
4	1	-0.5	0	0
4	2	-0.5	0.32	0

Table 4 Co-ordinates for Nozzle 3

ISSN: 2321-9653; IC Value: 45.98; SJ Impact Factor: 6.887
Volume 7 Issue II, Feb 2019- Available at www.ijraset.com

B. Geometry Construction

The above co-ordinate points are calculated from the formula (1).Co-ordinate points for the individual nozzle is imported into to the ANSYS geometry and the corresponding geometry is generated as shown in fig. 3.3.

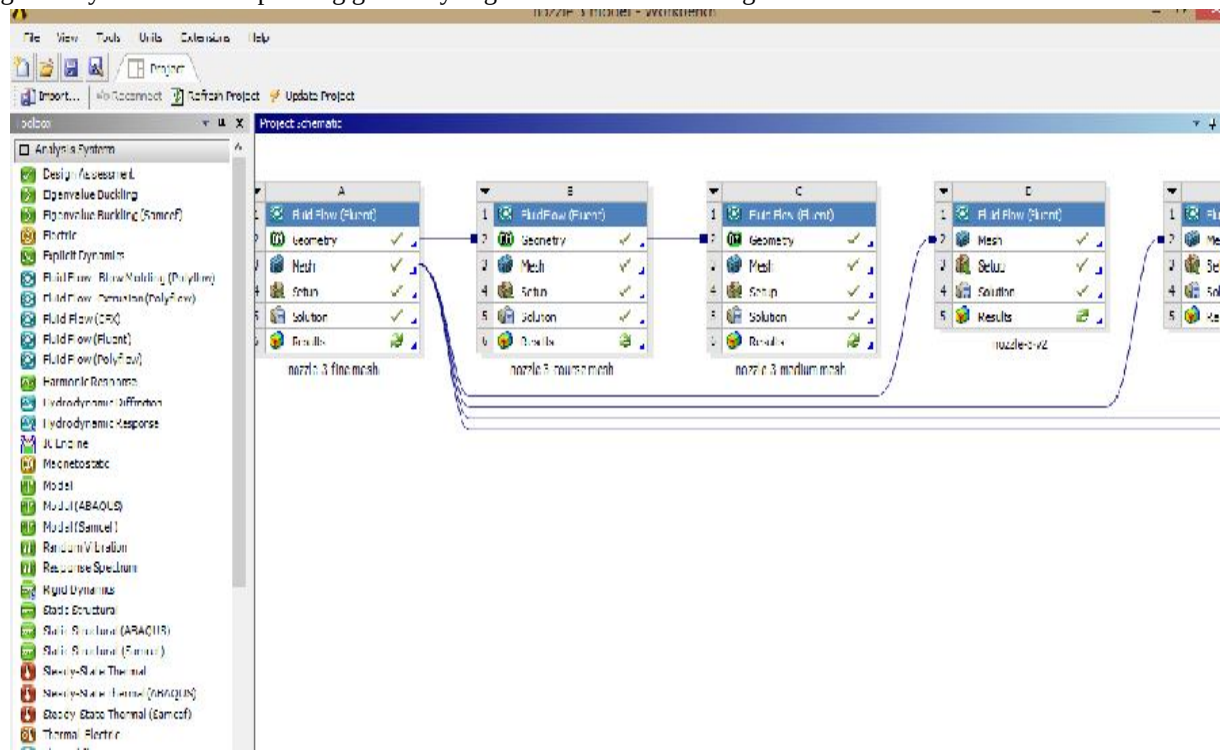

Fig. 3.2 Problem schematic for different nozzles

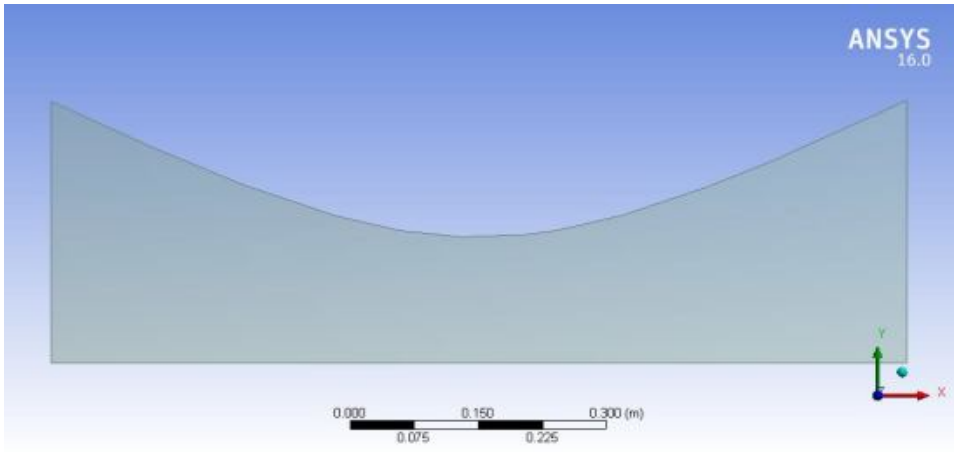

Fig. 3.3 Constructed axisymmetric geometry from imported co-ordinate points.

C. Mesh Generation

The fluid flow domain is completely discretized into grids. Grid generation is carried out by defining the structure of the fluid domain and the topology and later generating the grid over that topology. Here all cases of nozzle involve generation of mesh of structure grid type. The grid should exhibit some minimal grid quality as defined by measures of orthogonally (especially at the boundaries), relative grid spacing (15% to 20% stretching is considered a maximum value), grid skewness, mesh quality etc.

The below figures shows the difference between three different types of generated mesh i.e. Fine, Medium and Coarse for Nozzle-1 and the variation of number of elements in the grid results in better quality of the value during analysis which can be seen in the later stage of the experiment.

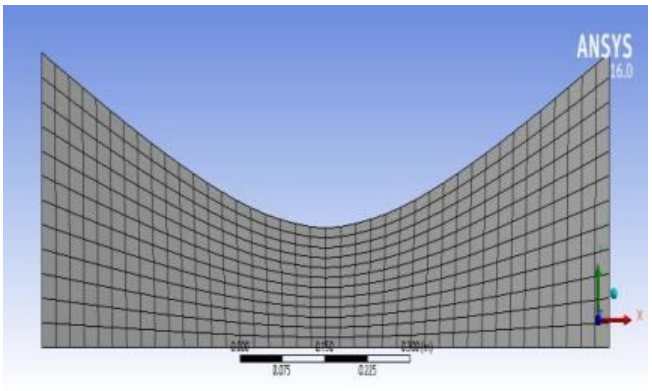

Fig. 3.4 Medium mesh generation

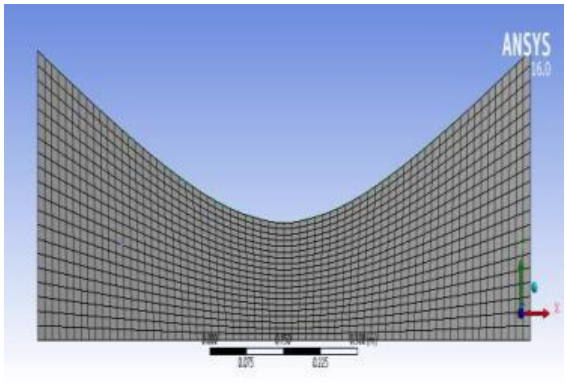

Fig. 3.5 Fine mesh generation

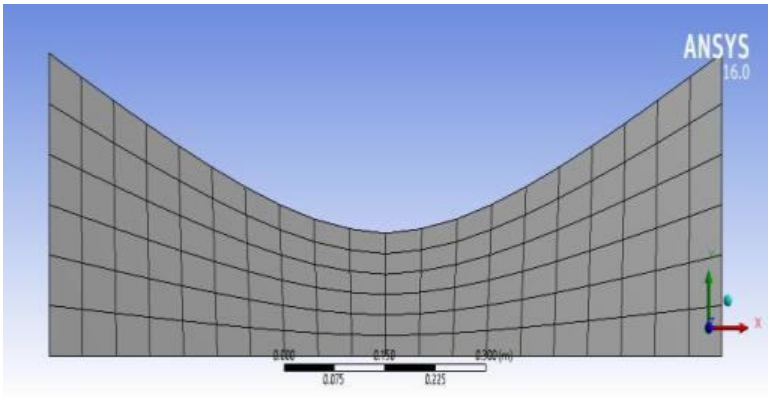

Fig. 3.6 Coarse mesh generation

D. Physics setup.

The objective for performing the simulation involves determining such things as the use of space-marching or time-marching, the choice of turbulence or chemistry model, and the choice of algorithms. Here we are using a density based solver and a k-epsilon turbulence model.

Here in this model analysis we use k-epsilon turbulence model and a density based solver as the objective involves solving the problem for a compressible flow.

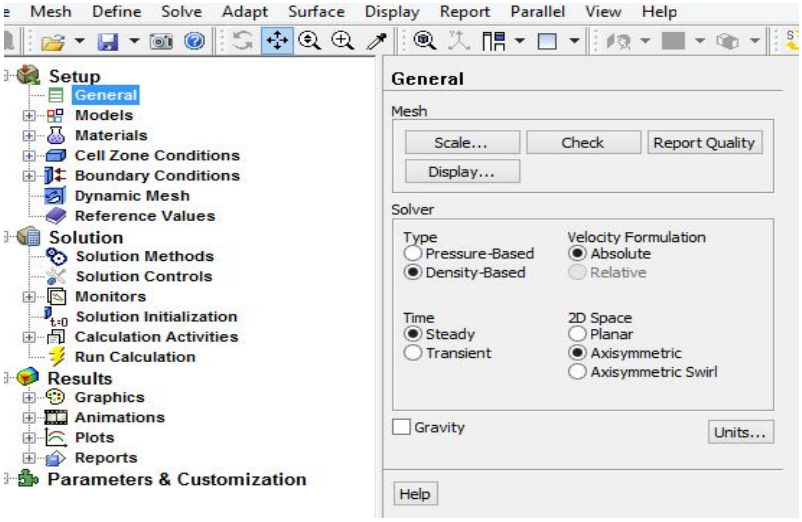

Fig 3.7 Setting Density-based type solver for the model

Since a finite flow domain is specified, physical conditions are required on the boundaries of the flow domain. The simulation generally starts from an initial solution and uses an iterative method to reach a final flow field solution. The given boundary conditions for our problem are as follows:

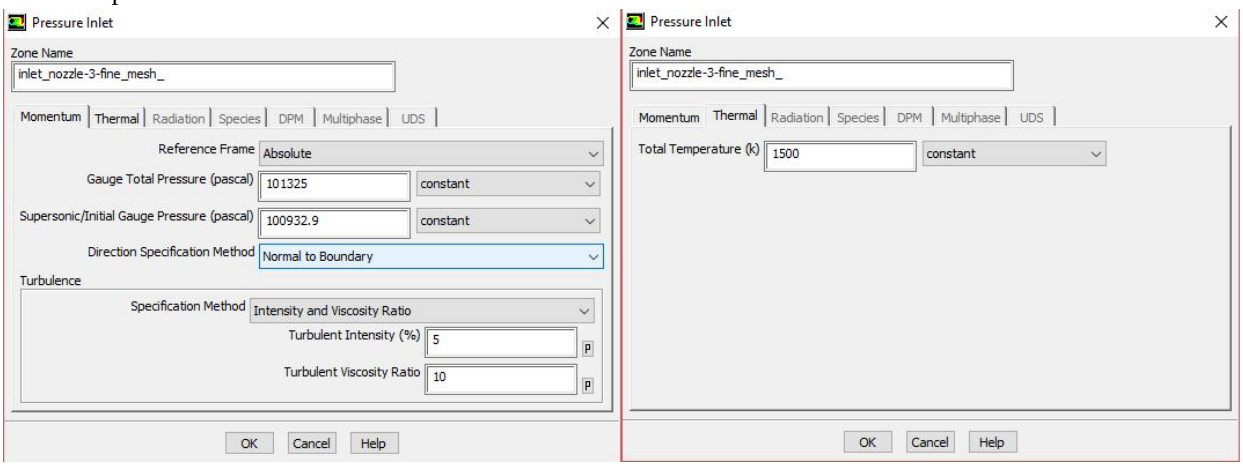

Fig. 3.8 Pressure inlet parameters for Boundary conditions

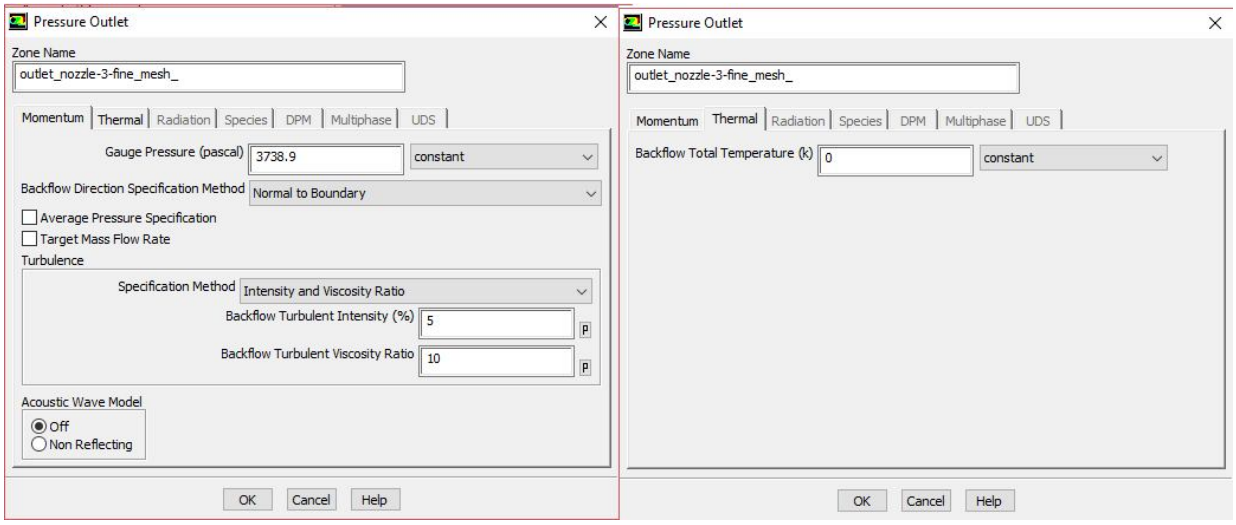

Fig 3.9 Pressure outlet parameters for boundary conditions

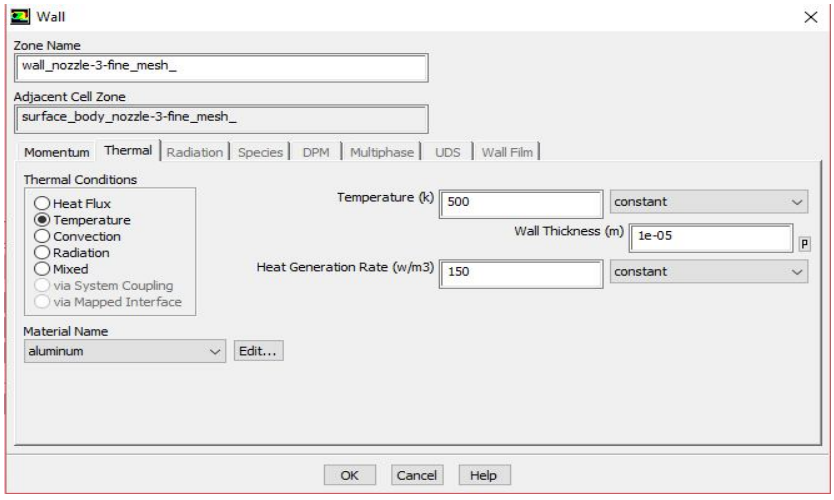

Fig. 3.10 Wall boundary conditions

The various input condition for all the 3 nozzles is tabulated in the below table with the respective boundary conditions. The variation of result for all these conditions is used as a vital statistical data for prediction in the R-Studio environment.

Table 5 values for the input varying parameters for all nozzles

V in m/s	Temperature in K	Boundary conditions		
35	500	(i)Inlet GTP-101325 IGP-98062.5 TI-5% TT-500	(ii)Outlet GP-3738.9 BFTI-5% BFTVR-10% BTT-0	(iii)Wall Stationary Wall No-Slip WT-100 Wt-1E-05 HGR-125
55	800	(i)Inlet GTP-101325 IGP-100614.5 TI-5% TT-1500	(ii)Outlet GP-3738.9 BFTI-5% BFTVR-10% BTT-0	(iii)Wall Stationary Wall No-Slip WT-125 Wt-1E-05 HGR-150
75	1200	(i)Inlet GTP-101325 IGP-10837.2 TI-5% TT-1200	(ii)Outlet GP-3738.9 BFTI-5% BFTVR-10% BTT-0	(iii)Wall Stationary Wall No-Slip WT-700 Wt-1E-05 HGR-300
85	1500	(i)Inlet GTP-101325 IGP-100932.9 TI-5% TT-1500	(ii)Outlet GP-3738.9 BFTI-5% BFTVR-10% BTT-0	(iii)Wall Stationary Wall No-Slip WT-300 Wt-1E-05 HGR-150

The fluent solves continuity, momentum and energy equation for the above properties simultaneously .It also solves the turbulence and scalar equations involved using the built in turbulence model functions. If the solution tends to converge it stops the iterations, if it doesn't then it re-iterates the process by updating the process to the begin stages and continues solving the equations until it converges. The fig 3.11 shows the working flow chart for convergence in fluent.

Fig. 3.11 Convergence criteria flowchart

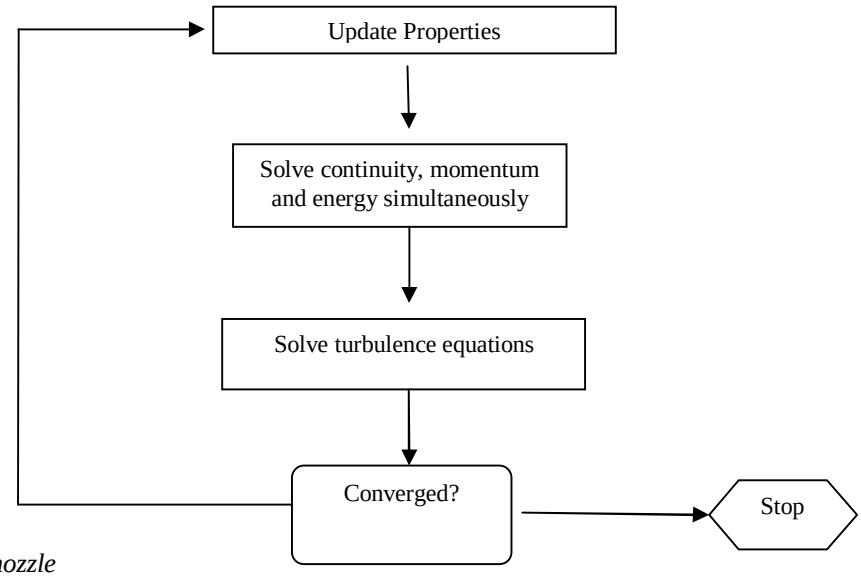

E. Flow variation in the nozzle

The different flow parameter contours for 3 different nozzles are shown below.

1) Nozzle – 1

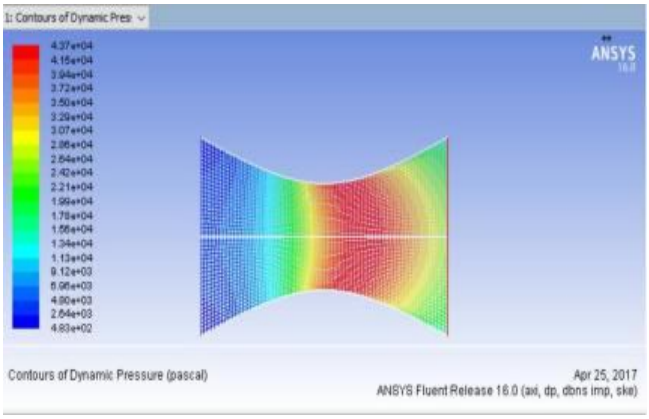

Fig. 3.12 Dynamic pressure contours

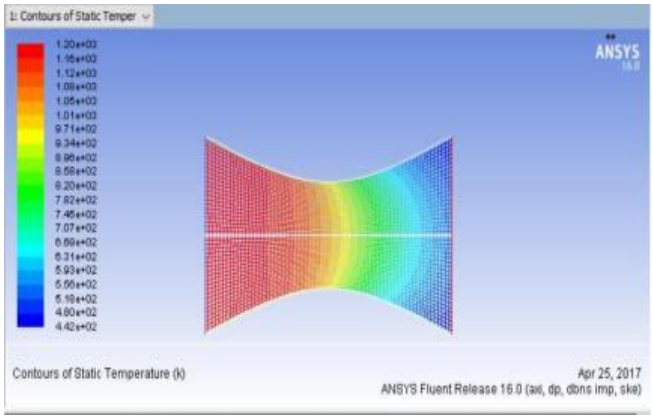

Fig. 3.13 Static temperature contours

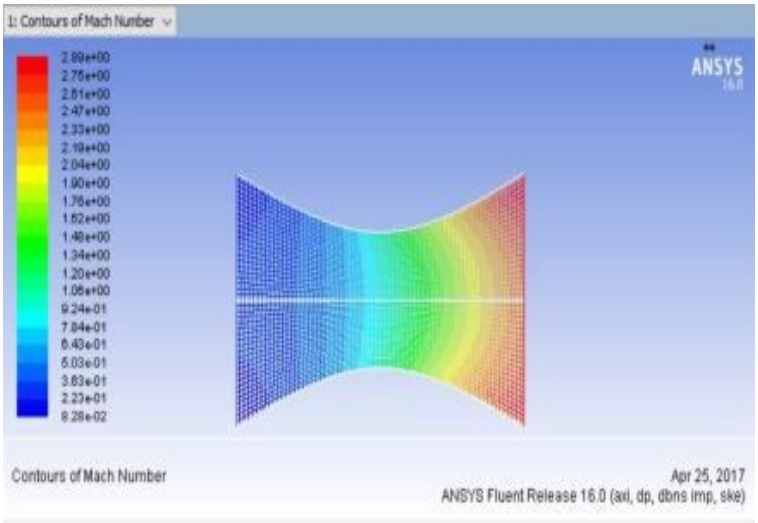

Fig. 3.14 Mach number contours

2) Nozzle – 2

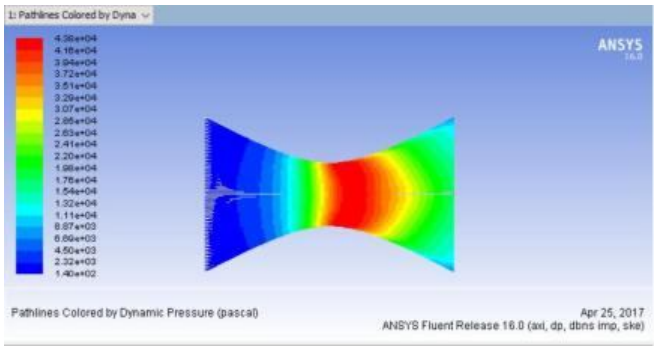

Fig. 3.16 Dynamic pressure contours

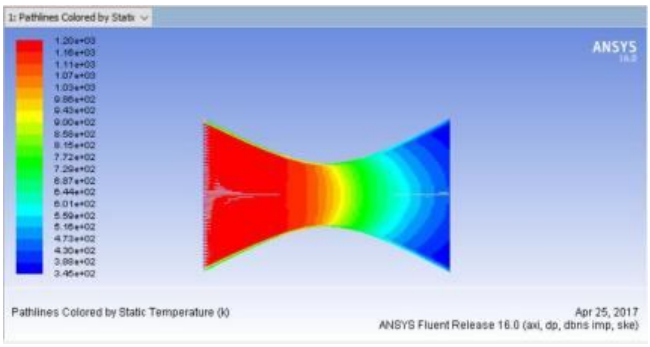

Fig. 3.17 Static temperature contours

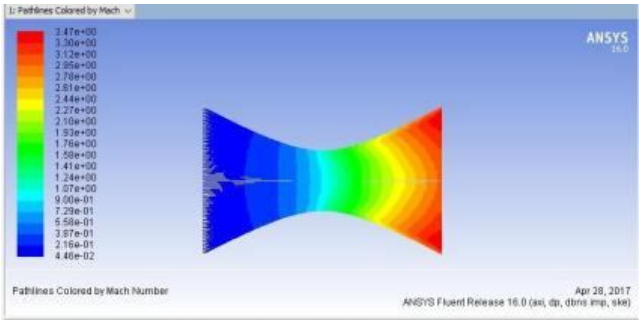

Fig. 3.18 Mach number contours

3) Nozzle – 3

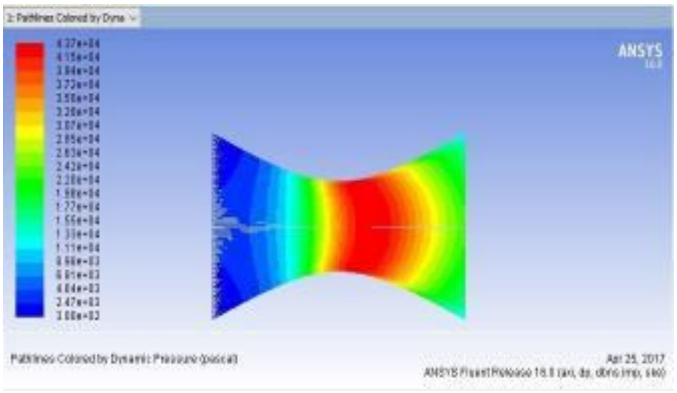

Fig. 3.19 Dynamic pressure contours

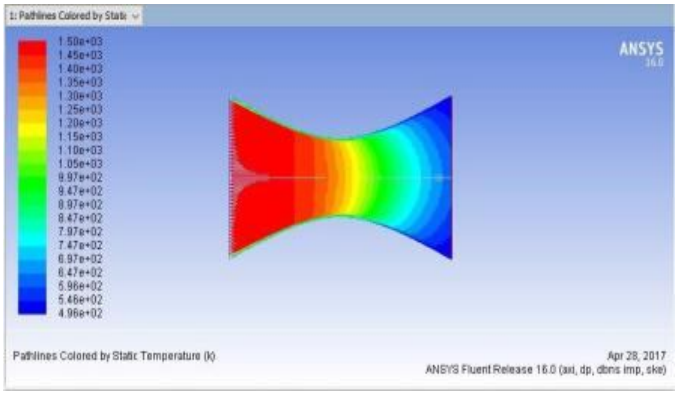

Fig. 3.20 Static temperature contours

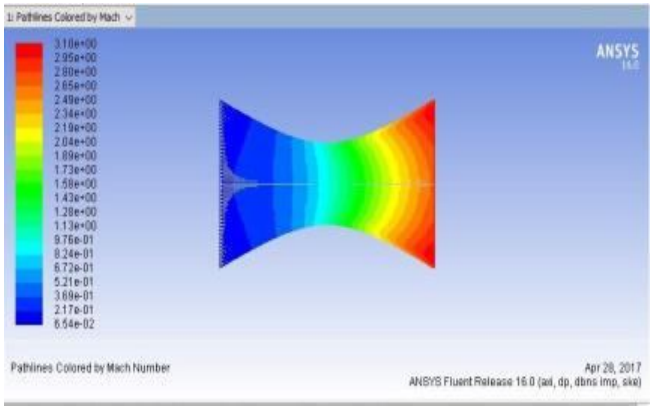

Fig. 3.21 Mach number contours

F. Grid independent Study

The accuracy in the result obtained for the above nozzles can be verified using a process known as grid independent study .Previously the various types of grids or the mesh generated is put into the analysis and individually for each mesh type the input parameters is applied listed in table 5.

One among the results obtained from grid independent study for nozzle – 3 is listed below in table 6.We can observe from the table 6 that the variation in the value is within the maximum allowed variation i.e. 5%. Hence we can manually verify that the analysis performed has a better mesh quality and the results obtained through analysis are correct.

Table 6 Variation in the P and ρ for different type of grid types

Mesh Type	P in Pascal	ρ in kg/m^3
Fine	4.32e+03	1.25e-01
Medium	4.30e+03	1.31e-01
Coarse	4.32e+03	1.27e-01

G. Exporting the data obtained to R-Studio in .csv format

Once the calculation is completed the required data is exported using the "WRITE TO FILE" option and selecting the required data in .csv format. Exporting it into .csv format is a crucial point as R-studio only imports data in only comma separated value format.

IV. PLOTTING ,PREDICTION AND OPTIMIZATION IN R-STUDIO

A. Plotting

Once the data is imported into the R –Studio platform the data can be stored by creating the inputted data inside a library. We can, for example following code to plot variations in r-studio:

```
>> X1<-read.csv ("MACHNUMBER.csv")
>> X2<-read.csv ("Location.csv")
>> Plot(X1~X2)
>> legend(locator(1),c("N1","N2","N3"),col=c("red","blue","green"),pch=c(21,22,24))
```

The variations of Mach number for different velocities mentioned in table 5 for all nozzles along the axis and along wall can be seen figure below.

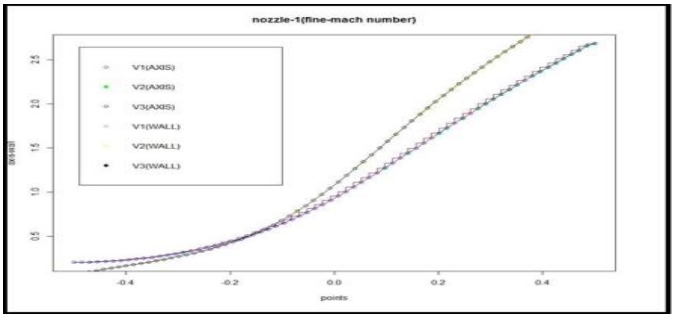

Fig 4.1 Variation along the nozzle axis and wall for 3 different velocities.

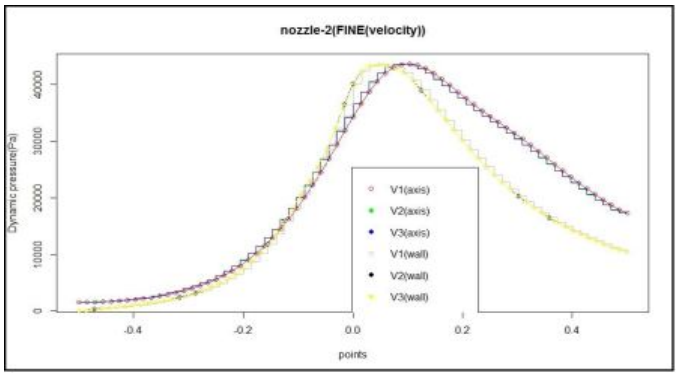

Fig 4.2 Variation of Dynamic Pressure for 3 different velocities along Nozzle 2

ISSN: 2321-9653; IC Value: 45.98; SJ Impact Factor: 6.887
Volume 7 Issue II, Feb 2019- Available at www.ijraset.com

The above plots show a typical variation Mach number at velocity 35, 55 and 75 m/s respectively along axis and wall of nozzle one having a throat to diameter ratio of 0.53and a fine mesh. Point ranging from -0.5-+0.5 corresponds to the length of the nozzle. What we observe that, at the converging portion of the nozzle for all the types of velocities there is a sudden increase in their Mach number or the velocity. So, it can be noted that our study can be more focused on the nozzle converging section primarily to predict the futuristic values.

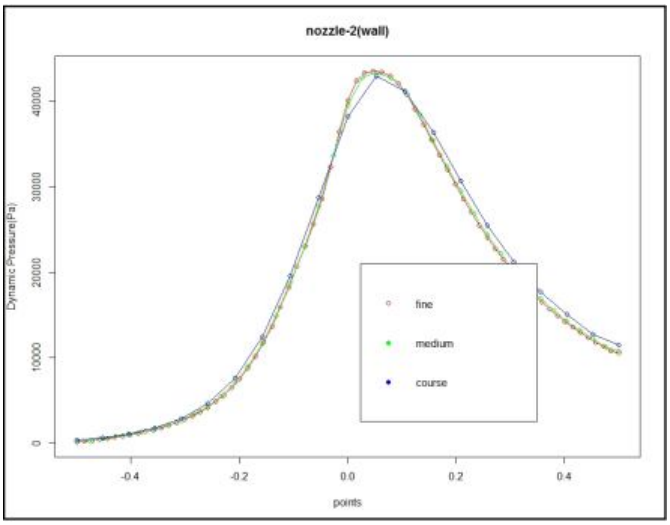

Fig. 4.3 Variation of Dynamic Pressure along the wall of nozzle 2 for different types of meshes

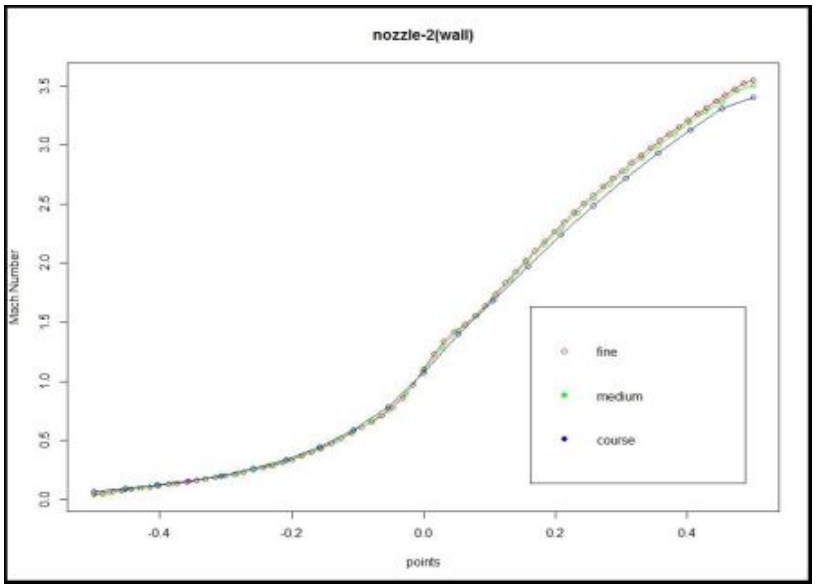

Fig 4.4 Variation of Mach number for Nozzle 2 along wall for 3 different types of meshes.

The above plots show the variation for nozzle 2 for throat to inlet diameter ratio of 0.40 and for 3 different types of velocity.
The corresponding variation of the dynamic pressure values are plotted against the location of the nozzle axis.
Similar to the previous variation, we see a decrease in the pressure at the diverging section of the nozzle, thereby once again focusing our study now on the diverging section of the nozzle.
Plots show the variation for nozzle 2 for throat to inlet diameter ratio of 0.40 and for 3 different types of velocity.
The corresponding variation of the dynamic pressure values are plotted against the location of the nozzle axis.
Similar to the previous variation, we see a decrease in the pressure at the diverging section of the nozzle, thereby once again focusing our study now on the diverging section of the nozzle.

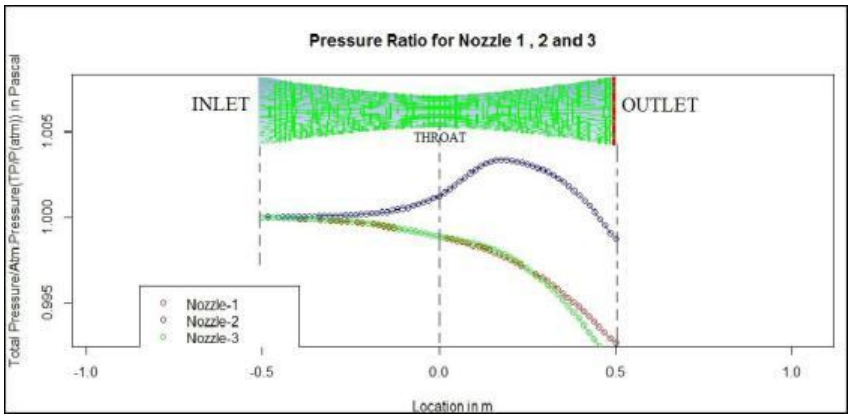

Fig. 4.5 Pressure ratio v/s the location along axis of all the 3 nozzles

A pressure ratio on the other hand gives us more information about the characteristics of the nozzle. Henceforth the above graph shows the total pressure to the atmospheric pressure ratio for the entire 3 nozzle. Nozzle 1 and Nozzle 2 having a moderate change in their pressure ratio gives us a clue about the stability of the flow within them. Nozzle 3 has a very rate of fluctuation in its flow and can be considered as a last option in the predictive section.

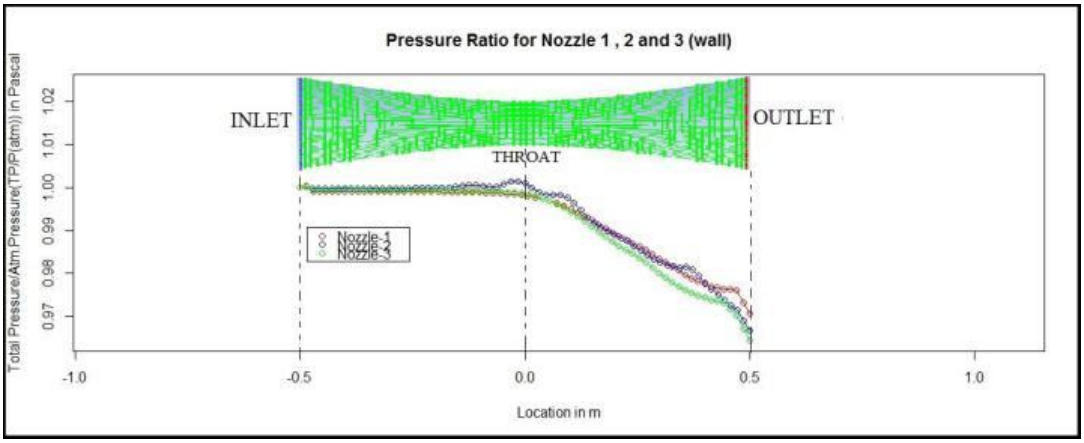

Fig. 4.6 Pressure ratio v/s the location along wall of all the 3 nozzles

When it comes to the convective heat transfer part, one of the important parameter includes the variation of properties along the wall of the nozzles. From the above plot, it's seen that the entire nozzle varies drastically beyond the diverging section of the nozzle.

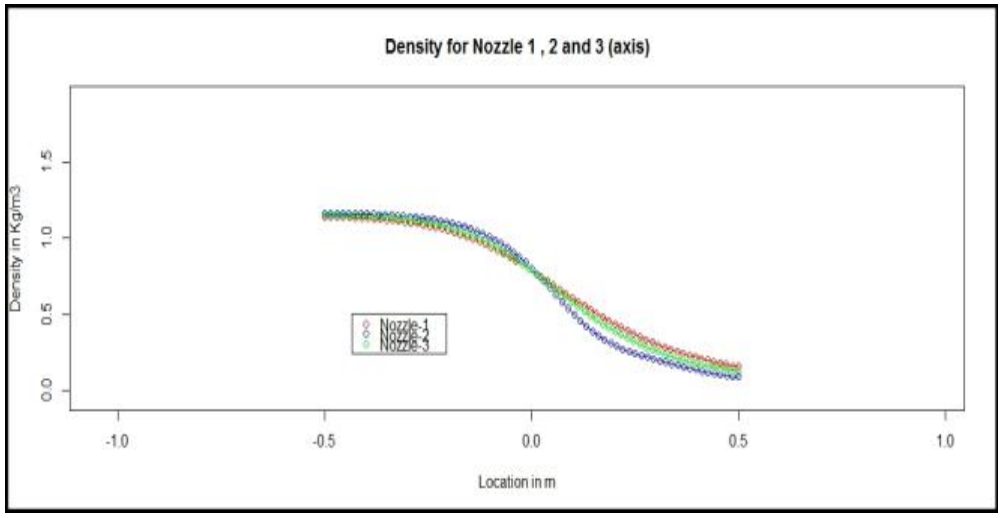

Fig. 4.7 Density variation along the nozzle axis for 3 different nozzles.

Density also varies along the throat for all three nozzles, the second figure showing an enlarged section on how these vary along the throat.

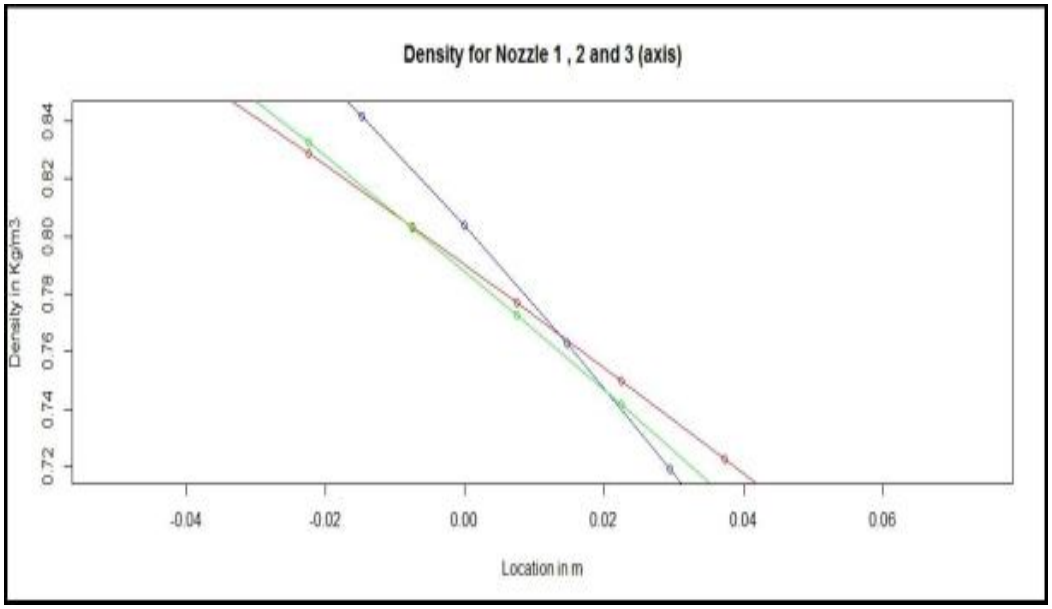

Fig. 4.8 Enlarged section of the variation

B. Prediction

1) Linear Regression

The general description of the regression models, the computing values for any regression model varies according to the type of the regression function you are using. A Simple linear regression model consists of a Independent variable from which we can Calculate the value Dependent variable. To understand this in a more efficient way, we will try to follow a simple procedure to Obtains the set of data what we need.

a) Step 1: Export the values from ANSYS® and try to look for the maximum dependent variable of which you want to predict the values upon

b) *Step 2:* Using the R-STUDIO® packages, Write the set of R-Codes for the dependent and for the independent variable.

c) *Step 3:* Repeat the values for 3 different set of input variables

d) *Step 4:* Compare the result obtained with the standard set of values and also with multiple regression and compute the percentage of error so obtained.

```
>> X1<-read.csv (Predicition1.csn)$Press
>>Y2<-read.csv (Prediction1.csv)$Temp
>>Relation<-lm (y2~x1)
>> PREDICTION<-data.frame(x1=7654)
>> RESULT<-predict (Relation, PREDICTION)
>> print (Result)
>> Summary (Relation)
>> plot (y2,x1,col="blue",main="Temperature vs
>> Pressure", abline(lm(x1~y2)),cex=1.3,pch=16,xlab="Pressure in pa",ylab="Temperature in k")
```

Where,

X1=Pressure values which have been imported from the “Prediction1” file exported from the ANSYS®, Y2= Temperature values which have been imported from the “Prediction1” file exported from the ANSYS® , Relation<-lm(Y2~X1)= establishes a relation between the values of temperature and pressure and inputs the variation of temperature according to the pressure values. , PREDICTION=Sets a Data Frame or an initial value of pressure for which we have to find the temperature value, in this case Pressure=7654 Pa, RESULT=Applies the function “predict ()” to calculate the value of temperature for the given value of Pressure.

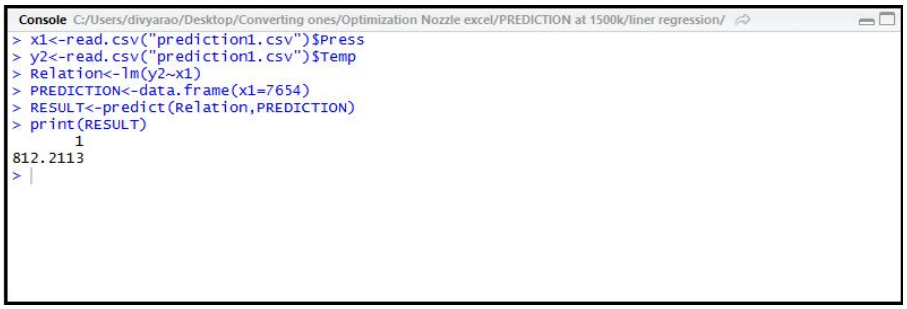

Fig. 4.9 Output for the input

Once we calculate different set of temperature for different input pressure, we verify that with the results obtained from the analysis to compute the percentage of error from table 7.

Table 7 Percentile difference in results from linear regression

From ANSYS	Pressure in Pascal	Temperature in Kelvin
	6.02e+03	6.71e+02
From R-Studio	Pressure in Pascal	Temperature in Kelvin
	6.02e+03	7.99e+02

Error %	19.076

2) *Multiple Regression:* Multiple Regression on the other hand is similar to linear regression but differs in the number of input values it can handle For example, in the previous regression model Pressure alone detected the value of temperature and the estimated value had an error of 19%, because the Temperature was completely dependent on Pressure i.e.

Temperature=f (Pressure)

But in the case of Multiple Regression this changes to:

Temperature=f (Pressure, Density, Velocity)

We write the following code to obtain the result using multiple regressions:

```
>> Table1<-read.csv (Predicition1.csn)
>> Density<-read.csv (Predicition1.csn) $Den
>> Pressure<-<-read.csv (Predicition1.csn) $Press
>> Velocity<-read.csv (Predicition1.csn) $Velo
>> Temperature<-<-read.csv (Predicition1.csn) $Temp
>> findout<-lm(Temperature~Velocity+Density+Pressure)
>> print (findout)
>> xpress<-coef(findout)[2]
>> xvel<-coef(findout)[3]
>> xden<-coef(findout)[4]
>> a<- coef(findout)[1]
>> x11<-6020
>> x22<-1290
>> x33<-0.0318
>> Y<-a+xpress*x11+xvel*x22+xden*x33
>> Print(y)
```

We later type in the following formula to obtain the temperature

Y = a + b1x1+b2x2+. . . .bnxn……. where Y is the responsible variable, a1,b1,b2 are the co-efficient and x1,x2,xn are predictor variables. Calling the summary function gives the input value for a, b1, b2.

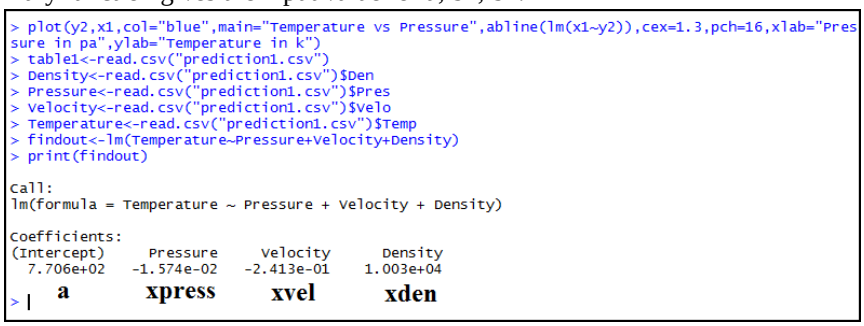

Fig. 4.10 Summary of the function and the variable needed for assigning the values

Continuing the allotment of shown variable to the formula mentioned fig 4.10

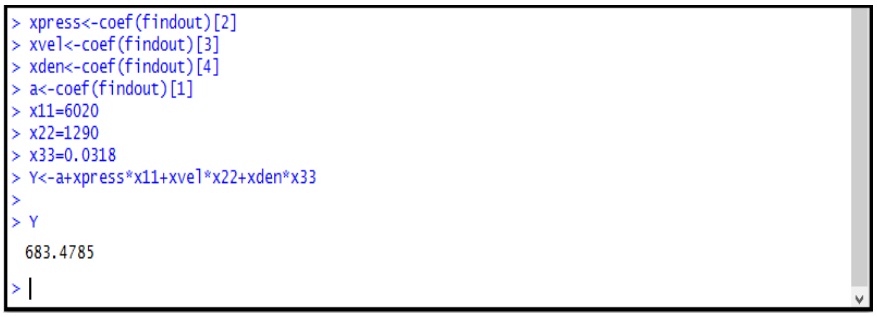

Fig. 4.11 Temperature value obtained by running the program

Thus, we could find that after running the program we see that the value of temperature obtained from the program and the value from R-STUDIO® has very less error, from the observation below table 8:

Table 8 Percentile difference in results from multiple regressions

From ANSYS	Pressure in Pascal	Temperature in Kelvin
	6.02e+03	6.71e+02
From R-Studio	Pressure in Pascal	Temperature in Kelvin
	6.02e+03	6.83e+02

Error %	1.788

C. Optimization

Consider a function f(x) of a vector x. Optimization problems are concerned with the task of finding x? such that f(x*) is a local maximum (or minimum). In the case of maximization,

>> x*= argmax f(x)

And in the case of minimization,

>> x* = argmin f(x)

Most statistical estimation problems are optimization problems. For example, if f is the likelihood function and x is a vector of parameter values, then x* is the maximum Likelihood estimator (MLE), which has many nice theoretical properties.

When f is the posterior distribution function, then x* is a popular byes estimator. Other well-known estimators, such as the least squares estimator in linear regression are optimums of particular objective functions. We will focus on using the built-in R function optim to solve minimization problems, so if you want to maximize you must supply the function multiplied by -1. The

Default method for optim is a derivative-free optimization routine called the Nelder-Mead simplex algorithm. The basic syntax is

>> optim(init, f)

ISSN: 2321-9653; IC Value: 45.98; SJ Impact Factor: 6.887
Volume 7 Issue II, Feb 2019- Available at www.ijraset.com

Where init is a vector of initial values you must specify and f is the objective function.
There are many optional argument– see the help file details .If you have also calculated the derivative and stored it in a function df, then the syntax is
>> optim(init, f, df, method="CG")
There are many choices for method, but CG is probably the best. In many cases the derivative calculation itself is difficult, so the default choice will be preferred.
$M_f = C_d A \sqrt{(k\rho_o P_o (2/k+1))}^{(k+1/k-1)}$
Where,
M_f = Mass flow rate in kg/s
C_d = discharge co-efficient
A = Discharge hole cross-sectional area, in m^2
$K = c_p/c_v$
ρ_o = real gas density at total pressure and total temperature ,in kg/m^3
P_o = Absolute upstream total pressure, in Pa
We will find the location of the throat ,the related pressure and density values for the same and reduce the above equation and find the minimum and maximum values for the density required for the choking to take place The same procedure is followed for the other 2 types of nozzle and optimize the result to obtain ,which nozzle Is better than the rest. Once we select the preferred values from the fluent, now we try to compute the values using the reduced value and the function
>> optim ()
The corresponding code for optimization is:
>> Optimizing<-function(x){
>> den<-x[1]
>>pres<-x[2]
>> 8.31*10^-3*(den*pres)^0.5
>> }
>>Optim(c(den=”0.154463172”,pres=”56226.3789”),Optimizing,method=”SANN”)

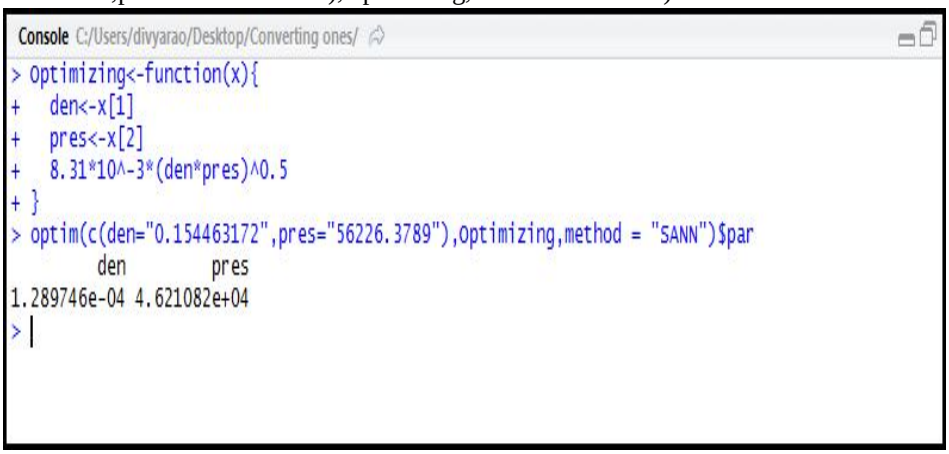

Fig. 4.12 Minimum and Maximum value for Density and Pressure

1) We find the minimum values to be
a) Density = 1.28 x 10^{-4} kg/m^3
b) Pressure = 4.6321 x 10^4 Pa
2) And the maximum value is found to be
a) Density = 1.55 kg/m^3
b) Pressure = 6.6321 x 10^4 Pa
The optimization is done for all three nozzles to find out which nozzle can be optimized according to the users need and the values are compared and tabulated in table 9.

	Nozzle - 1		Nozzle - 2		Nozzle -3	
	Pressure in Pa	Density in kg/ m^3	Pressure in Pa	Density in kg/ m^3	Pressure in Pa	Density in kg/ m^3
Minimum	5.66e+04	3.23e-04	5.93e+04	4.18e-04	4.62e+04	1.28e-04
Maximum	6.23e+04	2.024	6.74e+04	2.20	8.72e+04	1.57

From the above values we can look at the maximum and minimum set of values for 3 nozzles and according to the need of the operational stability we can choose the desired nozzle.

V. CONCLUSION

The primary objective of the project included the modelling of a nozzle having a compressible flow through it. The parameters included 3 different types of nozzles and analysing them for various conditions like grid independent study, different types of velocity and different types of temperature. For each type of conditions the analysis was carried out and the required data was exported. Going through the result gave us an example of how the flow was varying for different types of conditions. The flow variation images show how the flow varies from the inlet, experiences a drastic change in its parameters at the throat where the diameter reduces drastically and finally at the outlet. The objective is concerned more about the shock formation criteria of the nozzle. The Secondary objective included prediction and optimization of the obtained data and to find out which nozzle was suitable for a better shock characteristics. Prediction of the nozzle parameter using both linear regression and multiple regressions clearly gave information about the variable to be calculated but with a small numerical error. It was seen that increasing the input variables in a multiple regression function reduces the possibility of error formation. Optimization was needed to determine the best nozzle from all the results we obtained so far. Hence, taking into consideration for the future work, definitely the combination of ANSYS® and R-STUDIO® could basically provide us about the predicted and optimized calculations in a more convenient way than the conventional method. It's also evident that Non-Technical open software, R-STUDIO®, can also be used as Technical software to solve any type of flow problems.

REFERENCES

[1] J.N.B. Livingood, P. Hrycak, Impingement heat transfer from turbulent air jets to flat plates — A literature survey, NASA Technical Memorandum (NASA TM X-2778), 1970.
[2] H. Martin, Heat and mass transfer between impinging gas jets and solid surfaces, Advances in Heat Transfer 13 (1977) 1–60.
[3] K. Jambunathan, E. Lai,M.A. Moss, B.L. Button, A review of heat transfer data for single circular jet impingement, International Journal of Heat and Fluid Flow 13 (1992) 106–115.
[4] R. Viskanta, Heat transfer to impinging isothermal gas and flame jets, Experimental Thermal and Fluid Science 6 (1993) 111–134.
[5] R. Gardon, J. Cobonpue, Heat transfer between a flat plate and jets of air impinging on it, in: Int. Developments in Heat Transfer, ASME, 1962, pp. 454–460.
[6] R. Gardon, C. Akfirat, The role of turbulence in determining the heat transfer characteristics of impinging jets, International Journal of Heat and Mass Transfer 8 (1965) 1261–1272.
[7] R. Gardon, C. Akfirat, Heat transfer characteristics of impinging two dimensional air jets, Journal of Heat Transfer 88 (1966) 101–108.
[8] J.W. Baughn, S. Shimizu, Heat transfer measurements from a surface with uniform heat flux and an impinging jet, Journal of Heat Transfer 111 (1989) 1096–1098.
[9] P. Hrycak, Heat transfer from round impinging jets to a flat plate, International Journal of Heat and Mass Transfer 26 (1983) 1857–1865.
[10] D. Lytle, B.W.Webb, Air jet impingement heat transfer at low nozzle plate spacings, International Journal of Heat andMass Transfer 37 (1994) 1687– 1697.
[11] D.H. Lee, J. Song, C.J. Myeong, The effect of nozzle diameter on impinging jet heat transfer and fluid flow, Journal of Heat Transfer 126 (2004) 554–557.
[12] A.H. Beitelmal, A.J. Shah, M.A. Saad, Analysis of an impinging two dimensional jet, Journal of Heat Transfer 128 (2006) 307–310.
[13] J.H. Lienhard, Heat transfer by impingement of circular free-surface liquid jets, in: 18th National and 7th ISHMT-ASME Heat and Mass Transfer Conference, January 4–6, 2006.
[14] H.M. Hofmann, M. Kind, H. Martin, Measurements on steady state heat transfer and flow structure and new correlations for heat and mass transfer in submerged impinging jets, International Journal of Heat and Mass Transfer 50 (2007) 3957–3965.
[15] T.S. O'Donovan, D.B. Murray, Jet impingement heat transfer—Part I:Mean and root-mean-square heat transfer and velocity distributions, InternationalJournal of Heat and Mass Transfer 50 (2007) 3291–3301.
[16] T.S. O'Donovan, D.B. Murray, Jet impingement heat transfer—Part II:A temporal investigation of heat transfer and local fluid velocities, International Journal of Heat and Mass Transfer 50 (2007) 3302–3314.
[17] Y. Pan, J. Stevens, B.W. Webb, Effect of nozzle configuration on transport in the stagnation zone of axisymmetric, impinging free surface liquid

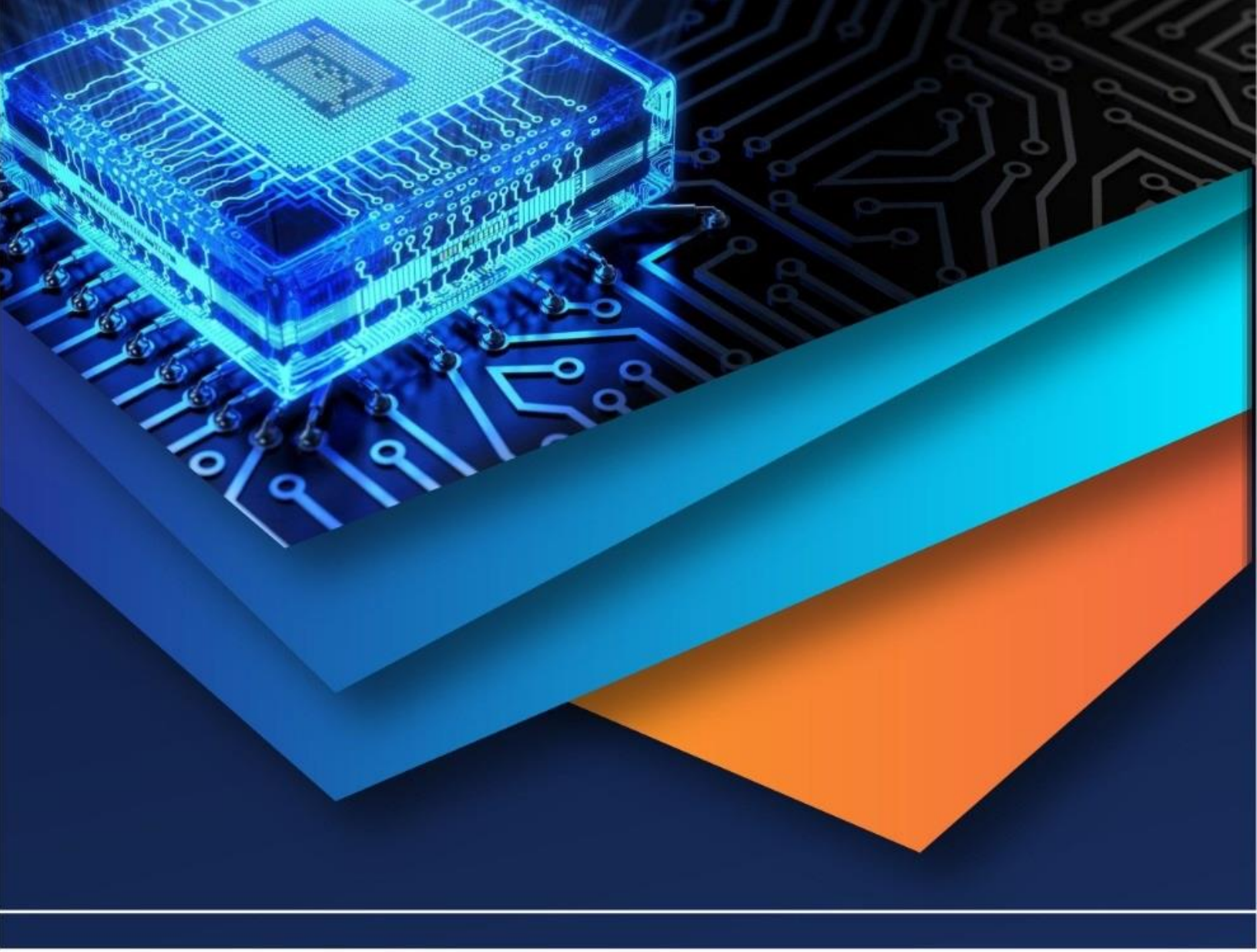

10.22214/IJRASET

45.98

IMPACT FACTOR: 7.129

IMPACT FACTOR: 7.429

INTERNATIONAL JOURNAL FOR RESEARCH

IN APPLIED SCIENCE & ENGINEERING TECHNOLOGY